THE AMERICAN SOCIETY OF MECHANICAL ENGINEERS
345 E. 47th St., New York, N.Y. 10017

94-GT-385

BEHAVIOR OF SEPARATION BUBBLE AND REATTACHED BOUNDARY LAYER AROUND A CIRCULAR LEADING EDGE

B. K. Hazarika and C. Hirsch
Department of Fluid Mechanics
Vrije Universiteit Brussel
Brussel, Belgium

ABSTRACT

The flow around a circular leading edge airfoil is investigated in an incompressible, low turbulence freestream. Hot-wire measurements are performed through the separation bubble, the reattachment and the recovery region till development of the fully turbulent boundary layer. The results of the experiments in the range of Reynolds numbers 1.7×10^3 to 11.8×10^3 are analysed and presented in this paper. A separation bubble is present near the leading edge at all Reynolds numbers. At the lowest Reynolds number investigated, the transition is preceded by strong low frequency oscillations. The correlation given by Mayle for prediction of transition of short separation bubbles is successful at the lower Reynolds number cases. The length of the separation bubble reduces considerably with increasing Reynolds number in the range investigated. The turbulence in the reattached flow persists even when the Reynolds number based on momentum thickness of the reattached boundary layer is small. The recovery length of the reattached layer is relatively short and the mean velocity profile follows logarithmic law within a short distance downstream of the reattachment point and the friction coefficient conforms to Prandtl-Schlichting skin-friction formula for a smooth flat plate at zero incidence.

NOMENCLATURE

C_p	Pressure coefficient
c_f	Friction coefficient
H	Shape factor; $[\delta^*/\theta]$
l	Length of the mean reverse flow region
Re_r	Reynolds number based on r and V
Re_x	Reynolds number based on x and V
Re_{xcr}	Critical Reynolds number
Re_θ	Reynolds number based on θ and U_e
r	Leading edge radius
s	Distance measured along the surface from the leading edge
t	Maximum mean thickness of the reverse flow region
U	Mean velocity
U_e	Velocity at the edge of the boundary layer
u	R. M. S. value of velocity fluctuations / Turbulence intensity
u^+	Velocity in wall units
u_τ	Friction velocity
V	Freestream velocity
x	Distance measured from the leading edge along the camber line
y	Distance from the surface
y^+	Distance in wall units
δ	Boundary layer thickness
δ^*	Displacement thickness
λ_θ	Pressure gradient parameter; $[(\theta^2/\nu)(dU_e/dx)]$
ν	Kinematic viscosity
θ	Momentum thickness

INTRODUCTION

Accurate prediction of flow field is the most important factor during the design of high performance gas turbine engines. To achieve this objective, one of the important phenomenon in need of more thorough study is the mechanism of boundary layer transition from laminar to turbulent flow and the reverse transition. Mayle (1991) identified three modes of transition; natural transition, bypass transition and separated-flow transition. The least understood of the three modes is the separated-flow transition. Hourmouziadis (1989), Mayle (1991), Walker (1992) and Walraevens and Cumpsty (1993) extensively discussed the role of separated-flow transition in turbomachines. The importance of the study of flow around a circular leading edge, to understand transition in turbomachines, is discussed by Walraevens and Cumpsty (1993).

The separation bubbles, normally occurring in gas turbines, are classified into two categories: (i) the short bubbles and (ii) the long bubbles {Mayle (1991)}. The effects of short bubbles on the flow field are mostly local. The long bubbles, on the other hand, have strong influence on the flow outside the separated region. The separation bubbles are in general unstable, small changes in the flow parameters may cause large changes in the bubbles. After re-examination of the limited amount of available data on separation bubbles, Mayle tentatively arrived at the conclusion that the shear layers above the long bubbles need a relatively large distance from the line of separation to the onset of transition. Once transition begins, the distance for completion of transition depends only on Re_θ at the point of separation. For low freestream turbulence (0.2% - 0.5%) Mayle gave correlations for onset and completion of transition of the shear layers. However, Mayle pointed out that these correlations are based on a small number of data available and are not sufficient to derive accurate correlations. Further experimental investigations are required for better understanding of the flow in the separation bubble formed over a continuous surface. Walker (1992) pointed out that the onset of transition does take place in the constant pressure region but does not have to complete before pressure recovery, the completion may occur even downstream of

Presented at the International Gas Turbine and Aeroengine Congress and Exposition
The Hague, Netherlands — June 13–16, 1994

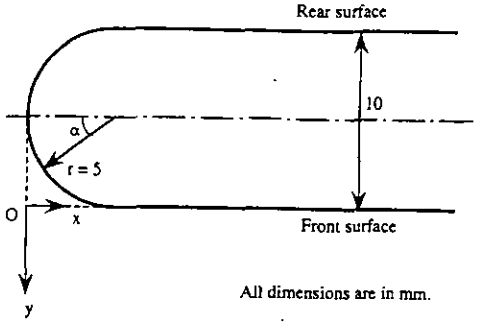

Pressure tap position on the leading edge (α)
Front surface: 0°, 15°, 30°, 45°, 60°, 75°, 90° (x = 5 mm).

Pressure tap position on the flat surface (x mm).
Front surface : 5, 7, 9, 17, 33, 65, 129, 257, 513, 1025.
Rear surface : 7, 9, 17, 33, 65, 129, 257, 513, 1025.

Figure 1. Schematic diagram of the plate leading edge.

the reattachment point. It is also pointed out that, in low freestream turbulence cases, the influence of upstream flow on the transition of separation bubble can not be ignored. Therefore, the characteristics of separation bubbles formed in the leading edge will be different from that in the mid-chord position.

Downstream of the reattachment region, rapid change in the flow field is expected due to the presence of the solid surface. Chandrsuda and Bradshaw (1981) investigated the flow behind a backward-facing step The investigations reveal that rapid decrease in the Reynolds stresses and the triple products take place because of the confinement of the large eddies by the solid surface. As a result, standard logarithmic law applies in the region close to the surface immediately downstream of the reattachment line. However, away from the wall the length scale of the free shear layer dominates the flow even far downstream of the reattachment. Therefore, in the recovery region the mean velocity profiles close to the surface follow the law of the wall but away from it the mean velocity profiles dip below the law of the wall curve because the length scale of the shear layer is comparatively large.

Walraevens and Cumpsty (1993) investigated flow separation in circular nose airfoils at various incidence, turbulence length scale and turbulence intensity. The lowest value of freestream turbulence intensity used in the measurements was about 0.5%. It is found that the effect of the turbulence intensity is significantly larger than the effect of Reynolds number on the separation bubble. The reattached boundary layer thickness is also found to decrease when the turbulence intensity is increased.

The need for more experimental investigations of flow in the separation bubbles is pointed out by various investigators. To develop correlations for use in turbomachines the experiments at high turbulence intensities are required. However, Walker (1992) has stated the need for experiments at low turbulence levels as, "*The authors and co-workers have found observations at low turbulence to provide useful physical insights, which have been beneficial in developing a more general understanding of transition phenomena*". The present work is carried out as a part of a large project in which the effects of leading edge shape, turbulence, shear, large eddy *etc.* on transition of the boundary layers in turbomachines are investigated. The investigation reported here is the first stage of this project in which the circular leading edge is investigated in a low turbulence freestream.

EXPERIMENTAL ARRANGEMENT, METHOD OF MEASUREMENT AND ANALYSIS, ESTIMATED ERROR

Experimental Arrangement

The experimental investigation is carried out in the VUB

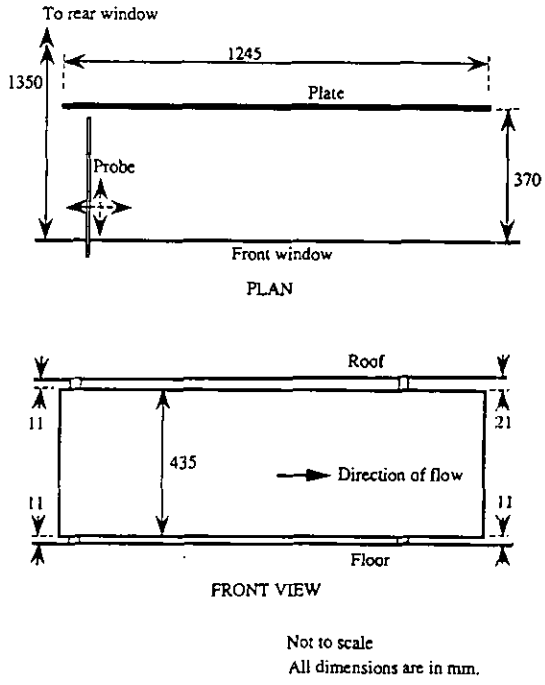

Figure 2. Schematic diagram of the plate set-up in the test section.

boundary layer tunnel, which is an open return tunnel driven by a centrifugal blower. The tunnel has a contraction ratio of 9.2; at the end of which, the cross section is 1350 mm wide and 450 mm high. The test section is 8 m long and has a flexible roof. The non-uniformity of the freestream in the test section is less than 0.5% and the turbulence level is less than 0.1%. A detailed investigation of the flow in the test section was reported by Hazarika and Hirsch (1991).

The flat-plate used for the experiment has 435 mm span, 1245 mm chord and is 10 mm thick. A schematic view of the leading edge of the flat plate is shown in Figure 1. The flat plate has a semicircular leading edge, which blends tangentially with the flat surfaces. There are 9 orifices of 0.5 mm diameter for static pressure measurement, on either side of the airfoil near mid-span. Most of these holes are clustered near the leading edge. In addition, the curved portion of the leading edge has 7 equispaced (15°) holes on the side where the measurements are taken. The roof of the test section is adjusted to give zero pressure gradient (sufficiently downstream of the reattachment point) on this flat-plate at the nominal velocity of 30 m/s. A schematic view of the arrangement is shown in Figure 2. Care is also taken to set the flat-plate in such a way that at this velocity, near the leading edge, there is practically no difference in the static pressure on either side of the flat-plate.

The measurements reported here are taken using a single sensor hot-wire probe connected to a constant temperature anemometer (CTA). The probe has 3 mm prong separation. The sensor length is 1.25 mm and diameter 5 μm and the rest of the wire along with the prongs are gold plated. Large scatter in the velocity and turbulence intensity in the separation bubble was observed in the measurements taken with a boundary layer probe. Therefore, a normal probe instead of a boundary layer probe is chosen so that the prongs are normal to the surface and create minimum disturbance in the shear layer. The total pressure measurements at the same stations are also conducted with a pneumatic boundary layer probe with wall thickness of 0.08 mm and the outside dimension of 0.24 mm x 0.78 mm. All the pressures are measured with a single transducer, connected to the holes through a Scanivalve driven by a step motor.

The two channel data acquisition system (DAS), used for these measurements, has a 16-bit processor and is set at ±4 volts span. The DAS is capable of finding average, R. M. S., correlation and power spectra of the input signals. On-line monitoring of the signals are also carried out with the help of an oscilloscope and a spectrum

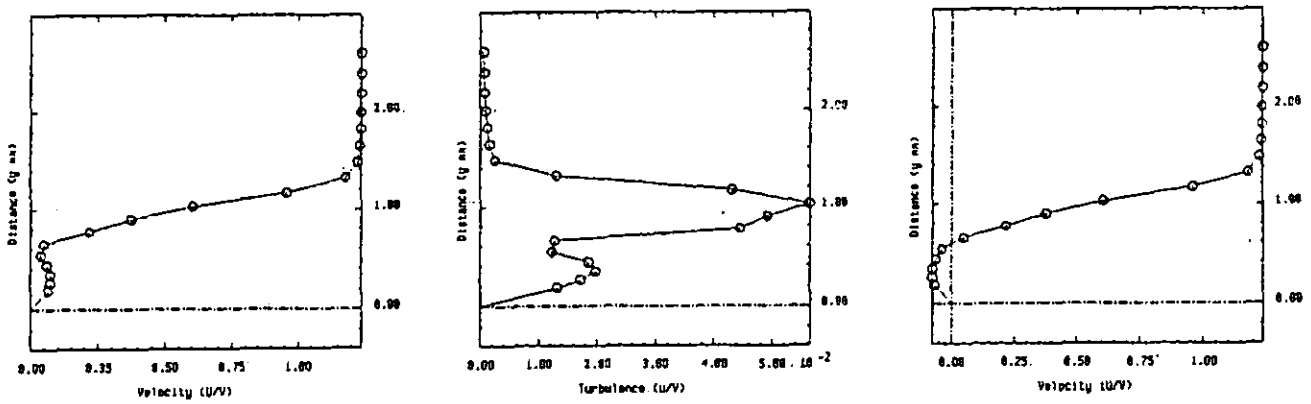

(a) Velocity profile before reverse flow region is identified.

(b) Turbulence intensity profile.

(c) Velocity profile after roverse flow direction is assigned.

Figure 3. Identification of reverse flow region for Re_r = 5030 at the traverse position x/r = 2.2

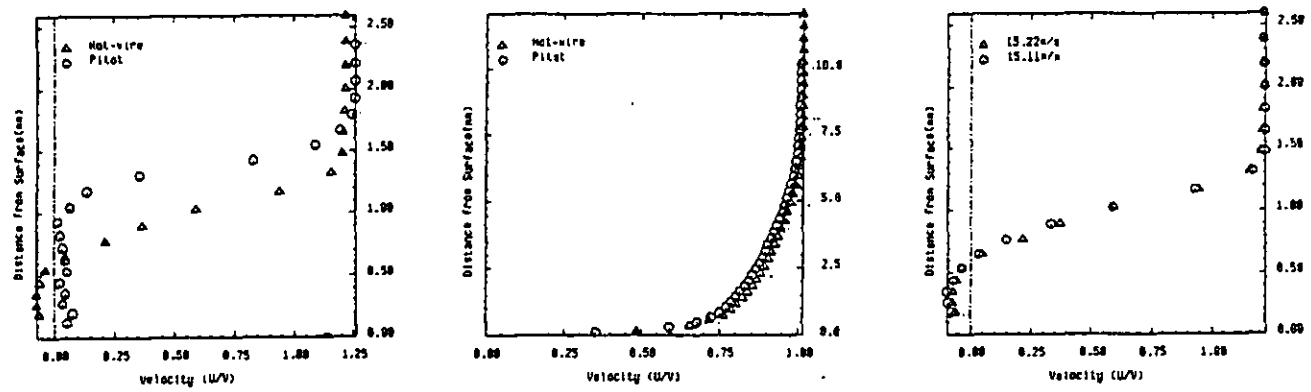

(a) Velocity profiles at x/r = 2.2 measured with the pitot and the hot wire probes.

(b) Velocity profiles at x/r = 19.2 measured with the pitot and the hot wire probes.

(c) Velocity profiles at x/r = 2.2 measured with the hot wire probe on two diffarant days.

Figure 4. Comparison of velocity profiles measured in the separated and the reattached regions for Re_r = 5030.

analyser. A personal computer co-ordinates the actions of all the step motor drives (Scannivalve and probe traverse), digital multimeter and the DAS. The personal computer is also used to convert some of the data before it stores them in a hard disc.

Method of Measurement and Analysis

The measured pressures are always expressed in terms of pressure coefficient before they are stored in raw data files. Far downstream of the leading edge (x/r > 50) the static pressure on the flat-plate remains constant. This constant value is taken as the reference static pressure. The freestream total pressure is the pressure measured by the orifice at the nose and the freestream velocity V is calculated from these values. All the velocity and turbulence intensity values are normalised with this value of freestream velocity. The static pressure variation over the flat-plate surface is measured before each traverse to confirm that the experimental arrangement did not change over time. It is found that 1% variation in freestream velocity did not bring about any detectable change in the variation of pressure coefficient over the flat-plate.

Hot-wire survey of the flow field is carried out at four nominal Re_r, $1.7x10^3$, $5x10^3$, $9.6x10^3$ and $11.8x10^3$. At each Re_r the measurements are repeated several times for reliability. In addition, the compensation for fouling and temperature variation (not necessarily linear) is incorporated with the help of reference readings taken every 20 minutes. The hot-wire probe is calibrated *in situ* before and after each experiment. King's law is used for calibration. The lowest uniform velocity achieved in this test section is around 1.2 m/s. The turbulence correction of the hot-wire data are performed by employing the method given by DeRuyck and Hirsch (1983).

When the hot-wire probe is traversed normal to the surface, across the separation bubble, kinks or discontinuities appear both on the mean velocity as well as on the turbulence intensity profiles as shown in Figure 3 (a) and (b). If the velocities measured below this point of discontinuity is assumed to be in the reverse flow region, a smooth velocity profile is obtained as shown in Figure 3 (c). The error in the velocity measured in the reverse flow region is comparatively large. The measurements are taken from about y = 0.2 mm and in most of the cases (outside the reverse flow region) it gives a value $y^+ > 5$, therefore, no attempt is made to correct the values for wall proximity effect.

At three Re_r, $1.7x10^3$, $5x10^3$ and $11.8x10^3$, the flow field is surveyed with the pneumatic boundary layer probe. To calculate the velocities the surface static pressure is assumed to be the stream pressure. A comparison of the profiles measured by the hot-wire and the pneumatic probe (pitot) across the separation bubble is shown in Figure 4 (a). The results from the pitot tube are not reliable in the separation bubble because of the large disturbances the probe creates in the bubble, the direction of flow and the large pressure gradient in the region. However, in the downstream of the reattachment point the results are quite close as seen in Figure 4 (b). Figure 4 (c) shows the velocity profiles through the separation bubble, measured by the hot-wire on two different days at the same nominal velocity, as a comparison for Figure 4 (a).

The reattached boundary layer profiles are compared with the universal log-law profile given below.

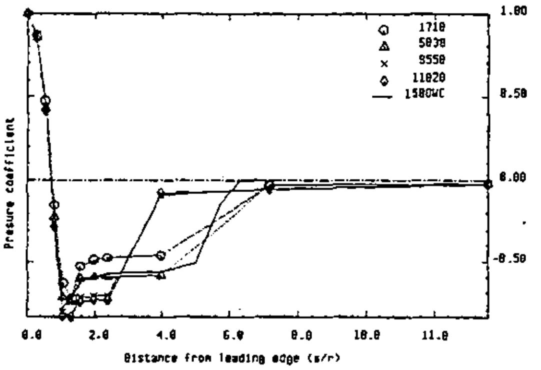

Figure 5. Variation of surface pressure coefficient for the range of Reynolds numbers investigated.

$$u^+ = 5.6 \log_{10}(y^+) + 4.9 \qquad (1)$$

The profiles are also compared with the expression given by Musker (1979) for turbulent boundary layer profile:

$$u^+ = 5.424\left(\tan^{-1}\frac{2y^+ - 8.15}{16.7}\right) + \left[\log_{10}\frac{(y^+ + 10.6)^{9.6}}{(y^{+2} - 8.15y^+ + 86)^2}\right] - 3.52 \qquad (2)$$

The flow fields, obtained from these measurements, are analysed using flow visualisation software {Vucinic *et al.* (1992)} to observe such features as the reattachment point, transition region *etc.* In this software the measured values of velocity and turbulence intensity are the inputs in the Cartesian co-ordinate system. These discrete values are the basis for linear interpolation describing the continuous field inside the cells. The continuous field thus obtained can be viewed in various ways like colour maps, iso-lines, cutting planes *etc.*

Outside the reverse flow region the velocity profiles measured by the hot-wire and boundary layer probes matched within 1%, confirming that the method of determination of position of the hot-wire sensor and the data are reliable. The measurements taken in the separation bubble with the hot-wire alone is considered reliable.

Estimated Error

The following are the uncertainties in the results for the confidence level of 99%.

The uncertainties in x and y positions are 0.04 mm or 0.8% of 'r' or the position whichever is larger.

The uncertainties in the velocity measured by the hot-wire are as follows:

0.6% of V for U > 5 m/s.

5% of U for U < 5 m/s.

10% of U for U ~ 1 m/s.

Can be as high as 50% for U < 1 m/s.

With the above uncertainties, the errors in the displacement thickness δ^* and the momentum thickness θ calculated for the profile shown in Figure 3 (c), can be as large as 3% and 25%, respectively.

The uncertainty in the R. M. S. value of the velocity fluctuations is 0.5% of V for U > 5 m/s.

Outside the separation bubble the uncertainty in the velocity measured by the pneumatic boundary layer probe is 0.5% of U for U > 6 m/s.

RESULTS AND DISCUSSION

The pressure coefficients around the circular leading edge and in the separation bubble are plotted for the four Reynolds numbers based on the leading edge radius (5 mm), namely, 1.7×10^3, 5×10^3, 9.6×10^3 and 11.8×10^3, are shown in Figure 5. The lines joining the points in this figure do not have any significance other than identifying the points for the same test conditions. The values are plotted against s/r to clearly show the variation along the leading

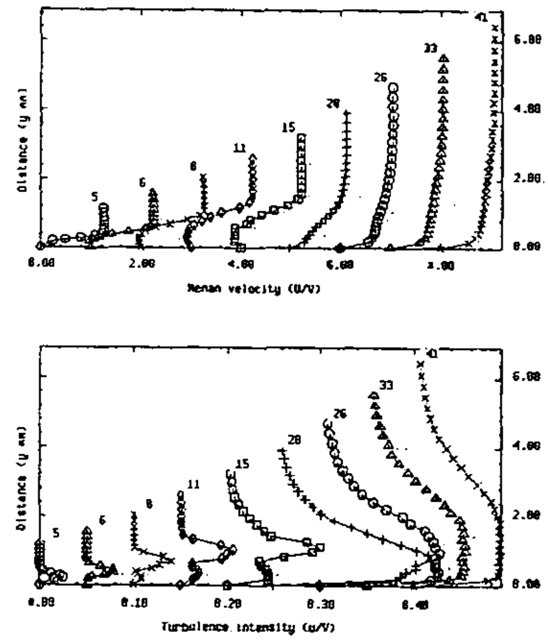

Figure 6 (a). Mean velocity and turbulence intensity profiles measured at Re_r = 5030.

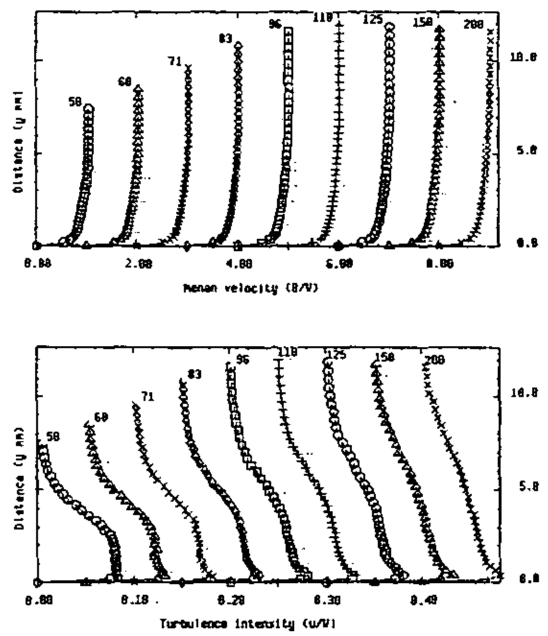

Figure 6 (b). Mean velocity and turbulence intensity profiles measured at Re_r = 5030.

edge. To compare these results with Walraevens and Cumpsty (1993) {will be indicated by WC, here on}, the pressure variation presented by them at 0° incidence (Figure 7, WC) is also plotted in this figure. It should be noted that the lowest turbulence level for the WC case was approximately 0.5%.

For all the cases shown here, the separation point is very close to the point where the curved surface meets the flat portion ($s/r = \pi/2$). Unfortunately, due to the limited number of static pressure holes in the region $2.5 < s/r < 7$, there is not enough measurements of pressure near the reattachment points. This obliterates the differences in the bubble length (if pressure variation is taken as the indicator) for the cases at the two lower and at the two higher Reynolds numbers. A clearer picture emerges when the pressure

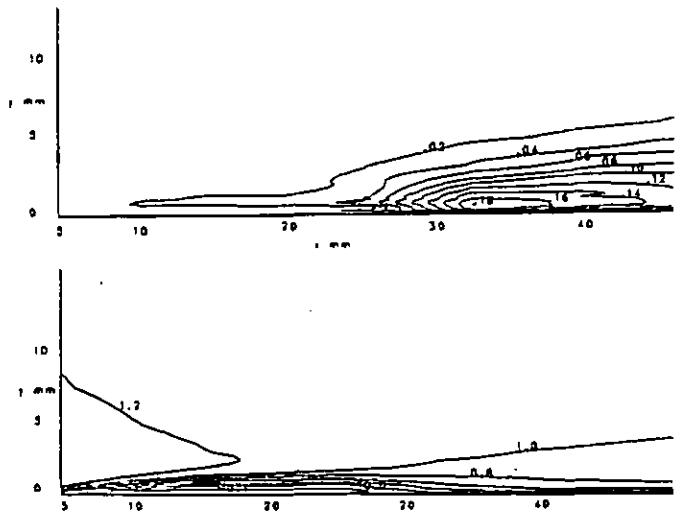

Figure 7 (a). Iso-lines of mean velocity (lower plot) and turbulence intensity (upper plot) near the leading edge at Re_r = 1710.

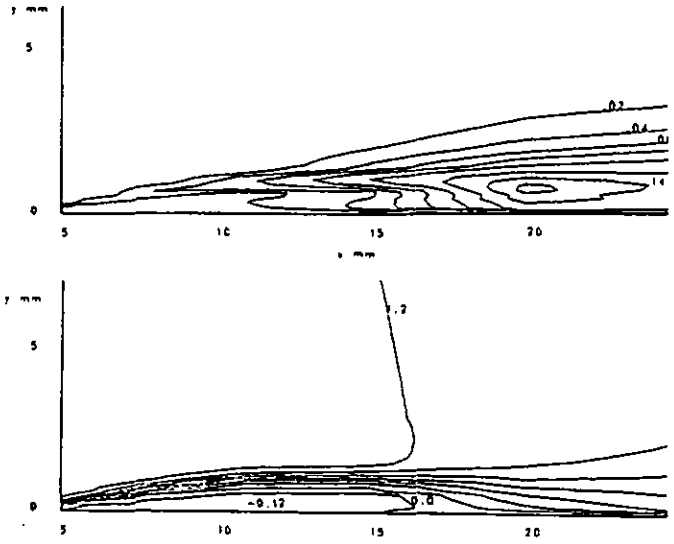

Figure 7 (b). Iso-lines of mean velocity (lower plot) and turbulence intensity (upper plot) near the leading edge at Re_r = 5030.

variation is examined in conjunction with the velocity field either analysed by flow visualisation software or variation of shape factor or momentum thickness of the measured boundary layer.

The increase in the magnitude of minimum pressure as well as that of the plateau with the increasing Reynolds number is clearly visible in the figure. As explained by Walraevens and Cumpsty (1993), the increased magnitude of suction peak is the result of thinner boundary layer that develops on the leading edge at higher Reynolds number. The higher value of suction peak results in steeper rise in pressure, the net result is an increase in the pressure gradient parameter λ_θ and the separation point moves upstream (this movement is very slight), this is the cause for creation of lower pressure in the separation bubble at higher Reynolds numbers. Walraevens and Cumpsty (1993) have also reported that the increasing turbulence level results in higher magnitude of suction peak and plateau and reduces the length of the separation bubble. The effect of turbulence level is also reported to be stronger than the Reynolds number. Therefore, it is normal that the pressure in the separation bubble at the Re_r = 1500 for WC is comparable with the pressure at Re_r = 5030 in this case.

The results of the hot-wire traverse at the nominal Reynolds number $5x10^3$ in the region from x/r = 1 to x/r = 40 are shown as carpet plots in the Figures 6 (a) and (b). In these four plots, the scales shown in the abscissa is true for the first (from left) curve in each plot. The distance of the traversing station from the leading edge (x mm) for each curve is shown at the top of the curve. The quantities (U and u) are presented as fractions of the freestream velocity (V) and the successive profiles are shifted by 1.0 for U/V and by 0.05 for u/V. On each curve a point is plotted at the zero value at y = 0 mm (a value not measured), to indicate no slip condition as well as the origin of the particular curve. The points at each station are joined by a continuous curve to indicate that they are from the same station. At this Reynolds number, the reverse flow is first detected at the station x/r = 1.2 (6 mm) and reattachment takes place between x/r = 3 (15 mm) and x/r = 4 (20 mm). The highest value of turbulence intensity in the flow field appears in the reattachment region (x/r = 4). In general the peak in the turbulence intensity coincides with the position of peak in the transverse gradient of velocity; except in the reverse flow and the recovery region. Due to the advection of highly turbulent flow from the reattachment point, in the reverse flow region (x = 8, 11 and 15 mm) a local maximum in the turbulence intensity appears where transverse gradient of velocity is very small. In the recovery region on the other hand, a plateau appears (x = 26, 33, 41 and 50 mm) close to the surface.

The iso-lines of the velocity and the turbulence intensity fields drawn using flow visualisation software at two Reynolds numbers, namely, $1.7x10^3$ and $5x10^3$ in the region close to the leading edge are shown in Figures 7 (a) and (b). In these figures the lines are drawn for U/V at 0.2 interval starting at 0. The lines for u/V start at 0.02 and they are drawn at 0.02 interval. The values of velocity and turbulence intensity at a few arbitrarily selected lines are also shown in these figures. The reverse flow zone stand out in the lower plot of Figure 7 (b). The length of the reverse flow region rapidly decrease with the increase in Reynolds number (the lower plots in the two figures). The turbulence intensity iso-lines in the flow field at these two Reynolds numbers show the outlines of the shear layer and the reverse flows. The long spikes projecting upstream in these figures show the centre of the shear layers where the peak values of the turbulence intensity occur. In these figures, advection of turbulence by the reverse flow is clearly visible from the smaller spikes below the longer ones. With the onset of transition the peak value of u rapidly increases. Due to the diffusive character of turbulent flow, downstream of completion of transition the turbulent region spread rapidly. This is reflected by rapidly diverging turbulence iso-lines downstream of 23 mm in Figure 7 (a) and 15 mm in Figure 7 (b), respectively.

The length of the reverse flow region, identified by the flow visualisation analysis, is plotted against Re_r in Figure 8 (designated HH). At lower Re_r the length of the reverse flow region reduces relatively rapidly with increasing Re_r, while the rate of change of length gradually reduces at higher values of Re_r. The solid line on this figure is drawn tentatively to show a probable variation of the length of the reverse flow region with Re_r. From the results presented by Walraevens and Cumpsty (1993) at 0° incidence, it was possible to roughly estimate two values of l/r, 4.9 at Re_r = 1350 and 4.1 at Re_r = 1500, these are also shown in this figure. Despite differences in the turbulence levels and errors iovolved in the estimation, the results of WC compare quite well with the present results. More experimental data are needed to examine whether at high Reynolds number the curve approaches zero or a non-zero constant value of l/r. Existing literature suggest that zero length of separation bubble is strictly possible at very large freestream turbulence case {Walker (1993)}, which is not the case in the present investigation.

The maximum thickness of the reverse flow region is relatively small at the lowest Re_r. Initially it increases with Re_r, seem to reach a peak value, and then gradually reduces. However, when the ratio of the maximum thickness and the length of the separation bubble is plotted against Re_r, a different picture emerges (Figure 9). The figure shows relatively rapid increase in thickness to length ratio at lower Re_r which subsequently level off at higher Re_r. Therefore, a

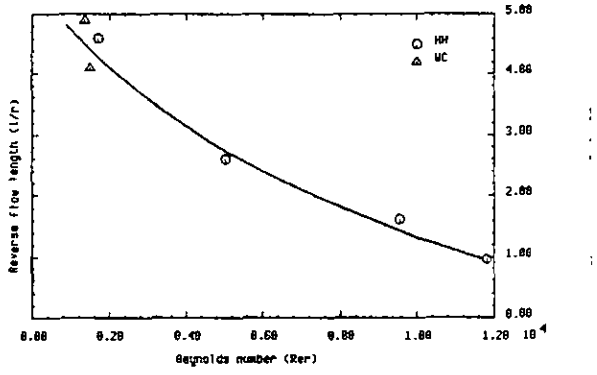

Figure 8. Variation of the length of reverse flow regions with Reynolds number.

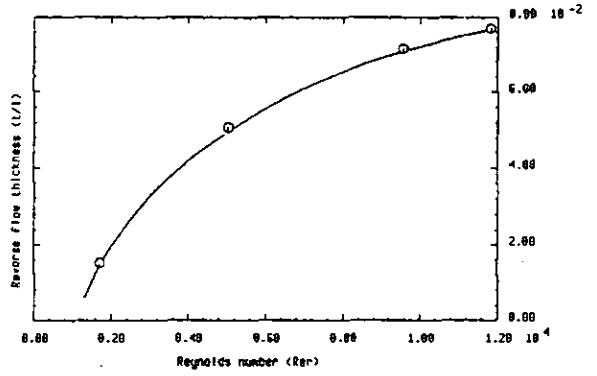

Figure 9. Variation of the thickness to length ratio of reverse flow regions with Reynolds number.

logical assumption is that the thickness to length ratio of the reverse flow region asymptotically approaches a constant value at higher Reynolds number as shown by the solid curve in the figure. Experiments at large numbers of Re_r values are required to verify these assumption.

The results of these experiments show that the separation point initially moves upstream with increasing Re_r. At the point of separation a point of inflexion on the velocity profile appears at y = 0. The point of inflexion moves away from the surface downstream of the separation point and the shear layer becomes more susceptible to transition. Since the transition to turbulence is promoted by the presence of point of inflexion on the velocity profile, once the Reynolds number exceed the stability limit, onset of transition may coincide with the point of separation and increase the ability of the flow to remain attached to the surface as a result the separation point will start to move downstream. This may be the reason why reverse flow is detected at the station x/r =1, in case of $Re_r = 9.6x10^3$ but not at $Re_r = 11.8x10^3$. The movement of the separation point can also explain why the thickness of reverse flow region increases with Re_r at lower values but reduces at the highest Re_r. From the variation of length and thickness to length ratio (Figures 8 and 9) of the reverse flow region with Re_r the following observations could be made. A short separation bubble will appear near the semicircular leading edge in a low turbulence incompressible flow at relatively high Reynolds numbers. The reverse flow region will grow longer and slender (t/l ratio will reduce) as Re_r reduces. At lower Re_r the bubble is formed by laminar separation and turbulent reattachment. At higher Re_r the transition in the shear layer may start at the point of separation.

At the lowest invesugated Re_r ($1.7x10^3$) the shear layer above the separation bubble show strong oscillations in the region of onset of transition. The results of spectrum of velocity fluctuation taken at two heights (y = 0.2 mm and y = 1 mm) at 3 traversing stations are shown in Figure 10. These results are presented following the suggestions given in Bradshaw (1971). Figure 10 (a) shows a spectrum taken in the reverse flow region. In this region relatively strong peaks in the spectrum appear at 150 Hz and 300 Hz. Figure 10 (b) shows a spectrum taken close to the centre of the shear layer at the same station. Here the dominant peak appears only at 300 Hz. Figure 10 (c) shows a spectrum taken in the reverse flow region, downstream of the point of onset of transition. In this region dominant peaks in the spectrum appear at 300, 375 and 450 Hz. The peak at 150 Hz is present but is smaller in magnitude than the dominant peaks. Figure 10 (d) shows a spectrum taken close to the centre of the shear layer at a station downstream of the point of onset of transition. The four peaks are also present in this spectrum. Closer to the surface, downstream of the reattachment point these peaks in the spectrum disappear rapidly. Figure 10 (e) shows a spectrum taken close to the surface in the reattached flow where no prominent peaks could be seen. However, away from the surface the peaks still appear in the spectrum as seen in Figure 10 (f). The peaks at 150 Hz is the dominant peak in this plot but the peaks at 300 and 450 Hz are also visible. In the reverse flow region the oscillations from the reattachment point is transported by the reverse flow, therefore they appear at upstream stations. This may have a feed back effect on the oscillation of the shear layer. The fluctuations in the frequency range between 150 Hz and 500 Hz are also observed at the freestream turbulence intensity 0.4% at a comparable Re_r by Goulas *et. al.* (1992). However, these fluctuations neither appear at higher freestream turbulence(1.2%) nor at higher Re_r. The flapping of the shear layer and the presence of large eddies are the probable cause of these peaks in the spectra. The oscillations at 150 Hz is comparable to the characteristic shedding frequency reported by Cherry, Hillier and Latour (1984).

Mayle's (1991) correlation is the most suitable for this series of measurements because of the extremely low level of turbulence in the freestream. The transition length of the separation bubble calculated from Mayle's (1991) correlation for short bubble and the features of the separation bubble found from these experiments are shown in Table 1. The predicted point of separation is taken from the result of a laminar Navier - Stokes simulation which shows separation just ahead of the blend point (88°). The separation point Re_θ needed for Mayle's correlation is taken as the experimental value measured immediately downstream of this point (at x = 5 mm). Following the usual practice the point of onset of transition is taken as the position where the peak value of u exceeds 25% of the highest value of u encountered in the flow field. From the experimental data it is found that the peak value of the turbulence intensity rapidly increases downstream of the onset of transition. The point of completion nf transition is taken as the position from which the iso-lines of turbulence intensity rapidly diverge in the flow visualisation analysis (Figure 7). The superscript '-' is used in this table to indicate position upstream of the measurement station. These data shnw that results comparable to Mayle's correlation is obtained only at low Reynolds numbers.

At all the four Re_r there is a sharp increase in momentum thickness θ across the reattachment point (Figure 11). To maintain clarity of the figure the variations at two Re_r ($1.7x10^3$ and $9.6x10^3$) are shown here. The increase in θ is fairly rapid through the recovery region, except at the lowest Re_r tested. For the flow at $Re_r = 1.7x10^3$ at the measurement station (x/r = 6.6) immediately downstream of the reattachment point Re_θ is found to be 160. At the last measurement station (x/r = 40), Re_θ becomes approximately 340 and continues to increase downstream. Murlis, Tsai and Bradshaw (1992) quoted that the lowest Reynolds number at which turbulent flow can be maintained (by a boundary layer) is given by Preston as Re_θ approximately around 320. Though at reattachment Re_θ is too small to sustain turbulent flow, the boundary layer remains turbulent and becomes a fully turbulent boundary layer downstream of the recovery region. At higher Re_r, $5x10^3$, $9.6x10^3$ and $11.8x10^3$, immediately downstream of the reattachment points the measured values of Re_θ are 350, 520 and 400, respectively. The results presented by Walraevens and Cumpsty (1993) for 0° incidence are also shown in Figure 11 (large scatter may be due to the inaccuracy in reading the data from the graphs), the general trend in growth of momentum thickness is in agreement with the present experiments.

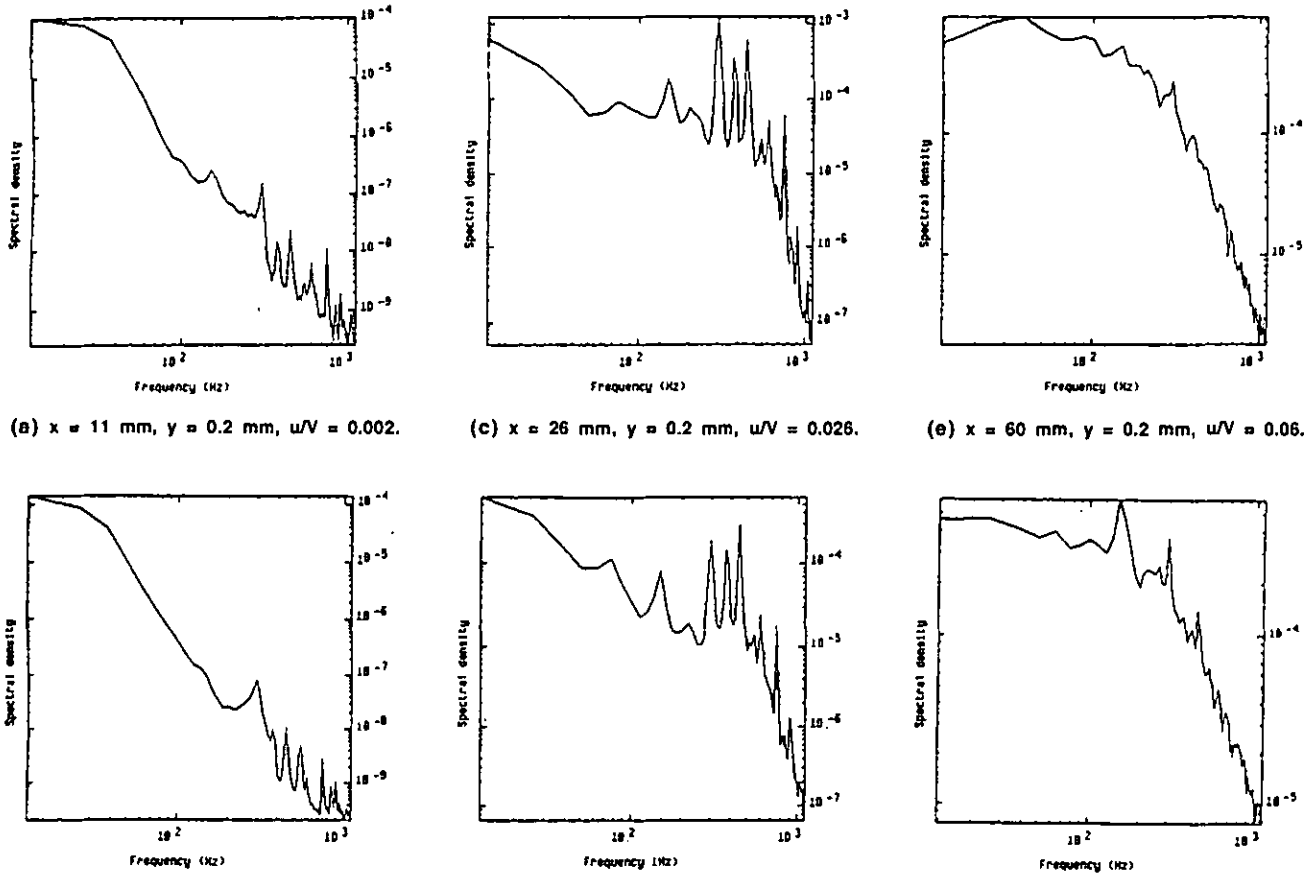

(a) x = 11 mm, y = 0.2 mm, u/V = 0.002. (c) x = 26 mm, y = 0.2 mm, u/V = 0.026. (e) x = 60 mm, y = 0.2 mm, u/V = 0.06.

(b) x = 11 mm, y = 1.0 mm, u/V = 0.02. (d) x = 26 mm, y = 1.0 mm, u/V = 0.04. (f) x = 60 mm, y = 1.0 mm, u/V = 0.105.

Figure 10. Frequency spectra taken in the reverse flow and in the shear layer for Re_τ = 1710.

Table 1. Features of the separation bubble.

Re_τ	Method of determination	Point of separation x (mm)	Point of onset of transition x (mm)	Point of completion of transition x (mm)	Point of reattachment x (mm)
1710	Experiment	6	20	26	28
	Prediction	5	13	23.5	-
5030	Experiment	5	11	15	17.5
	Prediction	5	9.5	16	-
9550	Experiment	5	8	11	12.3
	Prediction	5	8	11.5	-
11820	Experiment	5	6	8	9.5
	Prediction	5	7.5	10.5	-

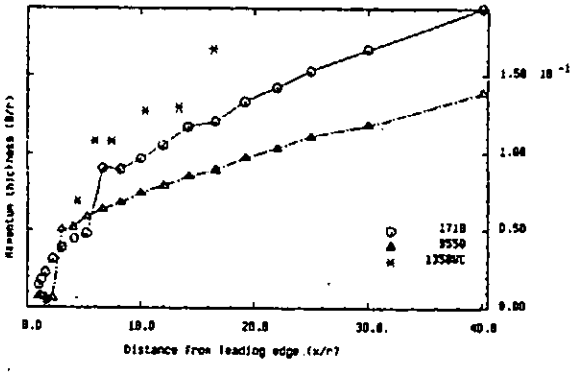

Figure 11. Variation of momentum thickness along the flat plate at Re_τ = 1710 and at Re_τ = 9550.

Across the reattachment line the shape factor drastically reduces at all Re_τ, to maintain clarity the variation at two Re_τ ($1.7x10^3$ and $9.6x10^3$) are shown in Figure 12. Within a short distance (of the order of the length of the separation bubble) downstream of the reattachment point, the shape factor attains a constant value (around 1.5). The slenderness of the reverse flow region at the lowest Re_τ is also reflected in this figure by the relatively low value of the shape factor in the separation bubble. The results presented by Walraevens and Cumpsty (1993) for 0° incidence, shown in this figure are in agreement with the present experiments. In the region where shape factor is constant, the variation of pressure is also negligible. Therefore, the friction coefficient is dependent only on the growth of momentum thickness.

The reattached shear layer follow the universal profile for the inner region of turbulent boundary layer, given by equation (1), within a short distance from the reattachment point. Four velocity profiles downstream of the reattachment point are shown in Figure 13 along with the universal profile (dotted) and Musker's expression (solid). In this figure the scale on the ordinate is true for the lowest plot, successive plots are shifted upwards from the previous plots by 5. The reattachment point for this case is at x/r = 5.6 (x = 28 mm); within a short distance, at x/r = 8.2 (x = 41 mm), the velocity profile is very close to the universal velocity profile even at a value of y^+ as small as 10. Such a close match is possible

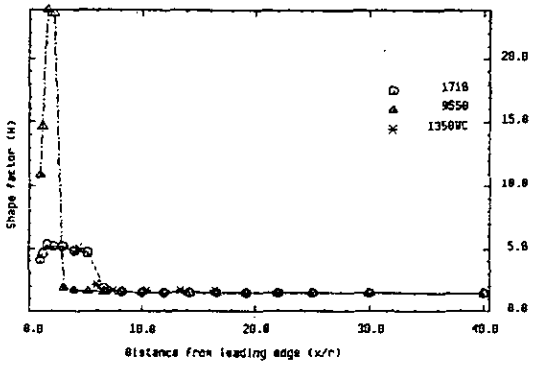

Figure 12. Variation of shape factor along the flat plate at Re_r = 1710 and at Re_r = 9550.

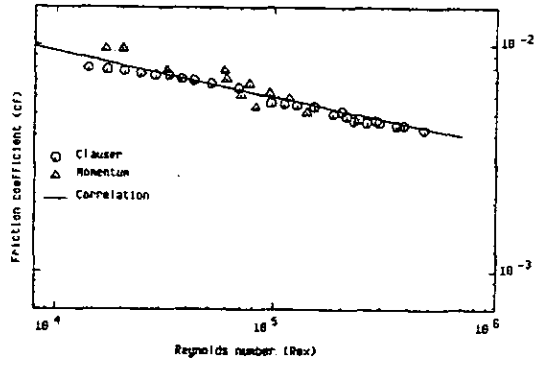

Figure 14. Variation of friction coefficient downstream of reattachment region.

so close to the reattachment because the length scale of the reattached shear layer happened to be quite close to y. It is seen from this figure that Clauser's method could be used to determine friction coefficient within a short distance downstream of reattachment point. In the recovery region, the velocity profile in the buffer layer is closer to the universal profile. At all Re_r, near the end of the measurement region (x = 200 mm) the velocity profiles follow equation (2).

Near the reattachment point, variation of θ and H are relatively rapid and Clauser method is inapplicable for determination of c_f. The friction coefficient found by using momentum integral equation in the recovery region is found to fall within ±15 % of the value given by the correlation $c_f = 0.0592\ Re_x^{-0.2}$. Downstream of the reattachment point, the variation of c_f with Rex, for all the four Re_r, is shown in Figure 14. The continuous line shown in this figure represent the variation of friction coefficient given by the correlation $c_f = 0.0592\ Re_x^{-0.2}$. This correlation is known to be valid for turbulent boundary layer in the domain $Re_{xcr} < Re_x < 5x10^7$, and is in agreement with Prandtl-Schlichting skin-friction formula for smooth flat plate at zero incidence {page 641, Schlichting (1979)}. For the reattached boundary layer it is found to be valid in the domain $1.4x10^4 < Re_x < 1.4x10^5$ (Figure 12). The relationship between Re_θ and c_f, given by Coles profile starts at the value Re_θ = 1500, only one value of Re_θ (1590, at x/r = 40 and $Re_r = 11.8x10^3$) is found to be suitable for comparison. At Re_θ = 1590 the experimental value of c_f (= 0.00425) is about 10% less than that given by Coles profile.

CONCLUSION

1. A leading edge separation bubble is formed on an airfoil with a semicircular leading edge at zero incidence in the low turbulence incompressible flow. At low Reynolds number the separation is laminar and reattached shear layer is turbulent. Thus, the transition

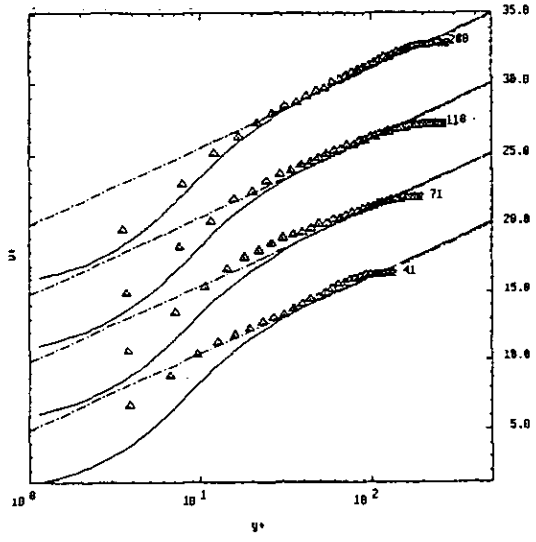

Figure 13. Mean velocity profiles downstream of reattachment at (x =) 41, 71, 110 and 200 mm for Re_r = 1710.

of boundary layer over circular leading edge airfoil is through separated-flow transition mode.

2. At low Reynolds number the transition of the separated shear layer is preceded by strong velocity fluctuations at discrete frequencies. These fluctuations are probably due to the presence of large eddies and flapping motion of the shear layer. The velocity fluctuations at discrete frequencies do not appear at higher Reynolds numbers.

3. The results of these experiments suggest that a short separation bubble will appear near the semicircular leading edge in a low turbulence incompressible flow even at high Reynolds numbers. The reverse flow region will grow longer and slender as the Reynolds number reduces. At higher Reynolds number the point of onset of transition and point of separation may coincide.

4. The reattached shear layer follows the universal log law prnfile within a short distance downstream of the reattachment point. Further downstream, the velocity profile below the outer layer closely follows Musker's (1979) correlation.

5. The variation of friction coefficient of the reattached boundary layer can be given by Prandtl-Schlichting skin-friction formula and is valid even in the recovery region.

ACKNOWLEDGEMENT

The investigations reported here was supported by CEC through a BRITE/EURAM project contract AERO-0002-C(TT).

REFERENCES

Bradshaw, P., 1971, "An Introduction to Turbulence and its Measurements", First Edition, Pergamon Press.

Chandrsuda, C. and Bradshaw, P., 1981, "Turbulence Structure of a Reattaching Mixing Layer", Journal of Fluid Mechanics, Vol. 110, p. 171.

DeRuyck, J. and Hirsch, Ch., 1983, "Turbulence Structure in the Boundary Layers of an Oscillating Airfoil", VUB-STR-14, Department of Fluid Mechanics, VUB, 1050 Brussels, Belgium.

Goulas, A., Nychas, S., Kastrinakis, E., Fotea, K. and Kyriakides, N., 1992, "Transition in Turbomachinery Flows - Cylindrical Leading Edge", BRITE/EURAM Project Contract No: AERO-0002, Faculty of Engineering, Aristotle University Thessaloniki, Greece.

Hazarika, B. K. and Hirsch, Ch., 1991, "Transition in Turbomachinery Flows", BRITE/EURAM Project Contract Report Nr. VUB-STR-17 , Department of Fluid Mechanics, VUB, 1050 Brussels, Belgium.

Hourmouziadis, J., 1989, "Aerodynamic Design of Low Pressure Turbines", AGARD Lecture Series 167.

Mayle, R. E., 1991, "The Role of Laminar-Turbulent Transition in Gas Turbine Engine", Trans. of the ASME Journal of Turbomachinery, Vol. 113, Part 4, p. 509.

Muralis, J., Tsai, H. M. and Bradshaw, P., 1982, "The Structures of Turbulent Boundary Layers at Low Reynolds Numbers", Journal of Fluid Mechanics, Vol. 122, p. 13.

Musker, A. J., 1979, "Explicit Expression for the Smooth Wall Velocity Distribution in a Turbulent Boundary Layer", AIAA Journal, Vol. 17, No. 6, p. 655.

Schlichting, H., 1979, "Boundary Layer Theory", Seventh Edition, McGraw-Hill Book Company.

Vucinic, D., Pottiez, M., Sotiaux, V. and Hirsch, C., 1992, "CFView - An Advanced Interactive Visualisation System based on Object-Oriented Approach", AIAA 30th Aerospace Science Meeting, Paper no. AIAA-92-0072.

Walker, G. J., 1993, "The Role of Laminar-Turbulent Transition in Gas Turbine Engines: A Discussion", Trans. of the ASME Journal of Turbomachinery, Vol. 115, Part 2, p. 207.

Walraevens, R. E. and Cumpsty, N. A., 1993, "Leading Edge Separation Bubble on Turbomachine Blades", ASME International Gas Turbine Conference, Paper no. 93-GT-91.